ChemMedChem

Chemistry Europe
European Chemical Societies Publishing

Accepted Article

Title: Benzimidazole Derivatives as Novel Zika Virus Inhibitors

Authors: Bui Thi Buu Hue, Phuong Hong Nguyen, Tran Quang De, Mai Van Hieu, Eunji Jo, Nguyen Van Tuan, Than Thi Thoa, Le Duc Anh, Nguyen Hoang Son, Danh La Duc Thanh, Myrielle Dupont-Rouzeyrol, Regis Grailhe, and Marc P Windisch

To be cited as: *ChemMedChem* 10.1002/cmdc.202000124

Link to VoR: https://doi.org/10.1002/cmdc.202000124

WILEY-VCH

WILEY-VCH

FULL PAPER

Benzimidazole Derivatives as Novel Zika Virus Inhibitors

Bui Thi Buu Hue,*[a]+ Phuong Hong Nguyen,[b,c]+ Tran Quang De,[a] Mai Van Hieu,[a] Eunji Jo,[b] Nguyen Van Tuan,[a] Than Thi Thoa,[b] Le Duc Anh,[a] Nguyen Hoang Son,[a] Danh La Duc Thanh,[a] Myrielle Dupont-Rouzeyrol,[d] Regis Grailhe,[e] Marc P. Windisch*[b,c]

[a] Dr. Bui Thi Buu Hue* (0000-0002-4635-933X); Dr. Tran Quang De, Mai Van Hieu (0000-0002-5077-2899); Nguyen Van Tuan, Le Duc Anh, Nguyen Hoang Son, Danh La Duc Thanh
Department of Chemistry, College of Natural Sciences
Can Tho University
Campus II, 3/2 street, Ninh Kieu District, Can Tho City, Vietnam
E-mail: btbhue@ctu.edu.vn

[b] Phuong Hong Nguyen; Than Thi Thoa; Eunji Jo; Dr. Marc P. Windisch*
Discovery Biology Division, Applied Molecular Virology Laboratory
Institut Pasteur Korea
696, Seongnam 13488, Republic of Korea

[c] Phuong Hong Nguyen; Dr. Marc P. Windisch* (0000-0003-1874-8503)
Division of Bio-Medical Science and Technology
University of Science and Technology
Daejeon 34141, Republic of Korea
Email: marc.windisch@ip-korea.org

[d] Dr. Myrielle Dupont-Rouzeyrol
URE Dengue and Arboviruses
Institut Pasteur de Nouvelle-Calédonie
98800 Noumea, New Caledonia

[e] Dr. Regis Grailhe
Technology Development Platform
Institut Pasteur Korea
696, Seongnam 13488, Republic of Korea

+These authors contributed equally to this work.

Supporting Information for this article is given via a link at the end of the document.

Abstract: We synthesized 50 benzimidazole (BMZ) derivatives with 1,2-phenylenediamines and aromatic aldehydes under mild oxidation conditions utilizing inexpensive, non-toxic inorganic salt sodium metabisulfite by one-pot condensation reaction and screened their ability to interfere with Zika virus (ZIKV) infection utilizing a cell-based phenotypic assay. Seven BMZs inhibited an African ZIKV strain with a selectivity index ($SI=CC_{50}/EC_{50}$) of 9-37. Structure-activity relationship analysis demonstrated substitution at the C-2, N-1, and C-5 positions of the BMZ ring were important for anti-ZIKV activity. The hybrid structure of BMZ and naphthalene rings was a structural feature responsible for high anti-ZIKV activity. Importantly, BMZs inhibited ZIKV in human neural stem cells, a physiologically relevant system considering the severe congenital anomalies, like microcephaly, caused by ZIKV infection. Compound **39** displayed the highest antiviral efficacy against the African ZIKV strain in Huh-7 (SI >37) and neural stem cells (SI=12). Compound **35** possessed the highest activity in Vero cells (SI=115). Together, our data indicate that BMZs derivatives have to be considered for the development of ZIKV therapeutic interventions.

Introduction

Zika virus (ZIKV) was declared a global health concern in 2016 by the World Health Organization. Over 2 billion people worldwide are at risk of contracting ZIKV, a member of the *Flaviviridae* family that was recently found to be responsible for a dramatically increased number of microcephaly cases and other congenital abnormalities in fetuses and newborns.[1] Additionally, ZIKV poses a health risk due to its association with neural-inflammatory diseases such as Guillain-Barré syndrome and ophthalmological complications in adults.[2] Furthermore, recent data demonstrate that the virus can be sexually transmitted by hiding in testes for long periods.[3] There are neither vaccines nor virus-specific therapeutics available to treat ZIKV-infected patients. To address this medical need, novel ZIKV interventions suitable for prevention and therapeutic purposes are urgently needed.

Benzimidazoles (BMZs) are recognized as a useful chemical scaffold for the development of pharmaceutical molecules of biological interest. BMZs have applications in diverse therapeutic areas, including anti-bacterial,[4] anti-fungal,[5] anti-histaminic,[6] anti-inflammatory,[7] and anti-HIV.[8] Additionally, BZMs were recently reported to be potent inhibitors of hepatitis C virus (HCV).[9] Yet, there are no reports of the activity of this type of compound against ZIKV, which belongs to the same viral family as HCV. Therefore, we designed and synthesized a series of BMZs and screened for their ability to inhibit ZIKV infection. One of the best documented methods for synthesizing BMZs is the condensation of o-phenylenediamine with aldehydes. Various reagents, including $NaHSO_3$,[10] $Na_2S_2O_3$,[11] $Na_2S_2O_4$,[12] and oxone,[13] have been utilized to promote this type of condensation. The use of $Na_2S_2O_5$ to construct disubstituted BMZs with two different functional groups at positions 1 and 2 of the BMZ ring has also been described, but this protocol requires the use of a toxic and high boiling point solvent such as DMF at a high

temperature for a prolonged reaction time.[14] In a previous study, we reported the synthesis of BZMs by a one-pot condensation reaction between 1,2-phenylenediamines and aromatic aldehydes under a mild oxidation condition utilizing inexpensive and non-toxic inorganic salt sodium metabisulfite.[15]

Based on this protocol, we report the design and synthesis of 50 1,2-disubstituted BZMs derivatives, including 29 new derivatives, and screened for their inhibition of ZIKV infection using a cell-based phenotypic high-content platform. This assay utilizes a multi-parametric readout to directly monitor viral replication in host cells, simultaneously evaluating cell viability to rapidly score compounds for activity. We also conducted a structure-activity relationship (SAR) study and further validated the antiviral activity of selected BMZs in human neural stem cells using an Asian ZIKV strain and by conducting mechanism of action studies.

Results and Discussion

Structural design and synthesis

Of the seven positions of the BMZ heterocycle, most anti-HCV BMZ-based compounds bear functional groups at the 1, 2, and 5 positions.[9c, 15-16] Considering these previous reports and the fact that ZIKV belongs to the same viral family as HCV, we devised strategies to synthesize a library of 1,2-disubstituted BMZs and screened for their anti-ZIKV activity. We changed the electron density of the pharmacophoric group by introducing bioisosteric groups, including the CF_3 group in the C-5 position and different aryl groups in the C-2 position, and substituting benzyl or alkyl groups at the N-1 position of the BMZ ring. Fifty structurally diverse 1,2-disubstituted BMZs (**1**-**50**), of which 29 were novel BMZ structures, were successfully synthesized with good to excellent yields (64-94%) based on a one-pot condensation reaction between N-substituted o-phenylenediamines 60 with substituted aromatic aldehydes 51-59 (Scheme 1).[15] The appropriate diamine **60** was readily prepared following reported procedures,[16] aldehydes **51**-**56** were obtained commercially, and aldehydes **57**-**59** were prepared via a tandem Stobbe reaction and cyclization starting from the corresponding substituted benzaldehyde.[17] In all cases, the reactions proceeded consistently and were completed within 2 h to generate the desired products with excellent isolated yields (78-94%). Only in the case of *N*-morpholinylpropyl *o*-phenylenediamines were longer reaction times (3-4 h) and lower yields (64-75%) observed (**9**, **10**, **16**-**19**, **44**) (Table S1).

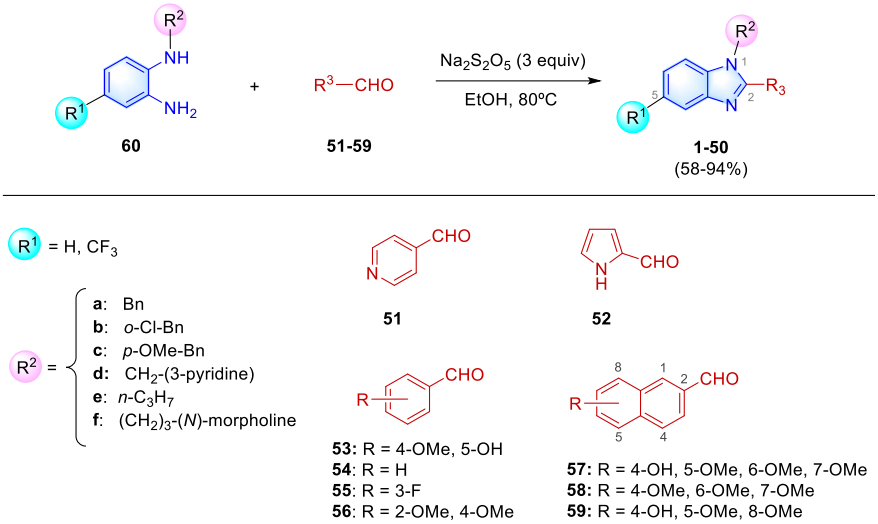

Scheme 1. Synthesis protocol of compounds **1**-**50**.

Evaluation of anti-ZIKV activity

Human hepatoma Huh-7 cell monolayers were treated with BMZ derivatives, mycophenolate acid (MPA), an immunosuppressant, used as a positive control, or vehicle (0.5% DMSO) for 1 h before infection with the African ZIKV strain MR766 with a multiplicity of infection (MOI) of 0.8 (Fig. 1A). Screening results are summarized in Table 1 (full data set of 50 BMZs presented in Table S1). Seventeen BMZs showed activity against ZIKV with a selectivity index (SI) >3. Of these, seven compounds (**23**, **24**, **30**, **32**, **34**, **35**, and **39**) exhibited high anti-viral activity with a SI>9. As shown in Fig. 1B, 76% of cells in DMSO-treated wells were infected compared with <1% of those treated with MPA, whereas the seven selected representative BMZs inhibited ZIKV to different extents at non-cytotoxic concentrations. Dose-response curve (DRC) analysis of the selected BMZs is shown in Fig. 1C. As BMZs are reported to have inhibitory effects on flaviviruses,[18] we evaluated the activity of the selected compounds against infectious HCV to determine compound specificity (Table S2). Of these, three derivatives (**23, 24,** and **35**) showed poor activity (SI<5), and one derivative (**39**) showed no anti-HCV activity.

Table 1. Anti-ZIKV activity of BMZ derivatives.

Compound	R_1	R_2	R_3	EC_{50} (μM)[a]	CC_{50} (μM)[a]	SI[b]
Category A						
3[e]	H	**b**	**53**	4.0±1.4	12.7±1.2	3.2
4[e]	CF_3	**b**	**53**	2.5±1.1	9.6±1.1	3.8
8[e]	CF_3	**d**	**53**	33.0±1.1	40.0±1.3	1.2
11	H	**a**	**54**	28.1±2.7	74.0±1.1	2.6
Category B						
20	H	**a**	**51**	53.3±5.7	97.9±51.1	1.8
21[e]	CF_3	**a**	**51**	61.4±1.1	82.6±1.3	1.3
22[e]	H	**b**	**51**	6.1±1.2	27.0±1.1	4.4
23	CF_3	**b**	**51**	24.7±2.0	>418	>16.9
24[e]	H	**c**	**51**	13.3±1.1	123.1±1.2	9.2
25[e]	CF_3	**c**	**51**	ND[c]	ND	NA[d]
28	CF_3	**e**	**51**	302.0±1.1	564.0±10.6	1.9
Category C						
30[e]	CF_3	**a**	**52**	7.5±1.1	146.0±1.3	19.5
32	H	**c**	**52**	18.5±1.1	263.0±1.2	14.2
33[e]	CF_3	**c**	**52**	8.5±1.3	18.0±1.6	2.1
34	H	**d**	**52**	48.3±1.3	684.5±1.2	14.2
35[e]	CF_3	**d**	**52**	6.1±1.2	55.5±1.2	9.1
36	CF_3	**e**	**52**	21.0±1.3	75.0±1.0	3.5
Category D						
37	H	**a**	**57**	~30.0	57.1±1.5	~1.9
39	H	**b**	**57**	1.9±1.0	70.9±1.4	37.3
40	CF_3	**b**	**57**	16.9±1.4	87.7±1.1	4.6
45	CF_3	**a**	**58**	2.5±0.7	2.6±0.8	1.0
46	H	**b**	**58**	10.0±1.3	19.3±1.1	1.9
48	CF_3	**d**	**58**	3.6±2.5	4.0±1.6	1.1
MPA	/	/	/	0.8±0.1	>150.0	>35.0

[a]EC_{50} and CC_{50} values were calculated by 10-point DRC analysis in triplicate. Experiments were repeated at least two times independently. [b]SI = CC_{50}/EC_{50}. [c]ND, not determined. [d]NA, not applicable (compounds were tested but CC_{50} and EC_{50} values could not be calculated). [e]Compounds were previously synthesized and published. See the experimental section. A full data set for the 50 BMZs can be found in the Supporting Information.

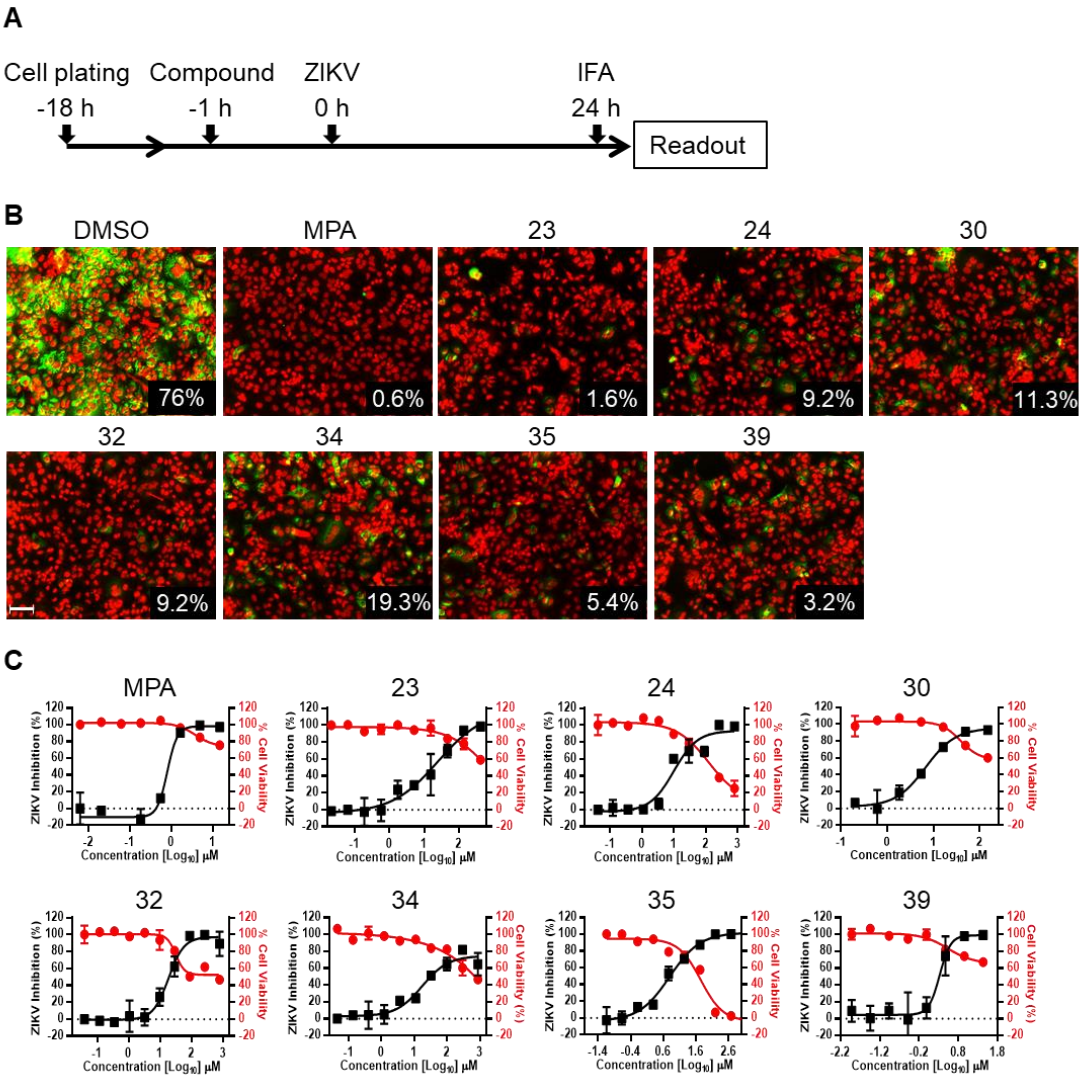

Fig. 1. Screening of BMZs for anti-ZIKV activity. (A) Screening schedule. Huh-7 cells were plated in 384-well format for 18 h prior to pre-treatment with serially diluted BMZs with a 3-fold serial dilution for 1 h (t = -1 h) before inoculation (t = 0 h). Cells were infected with ZIKV for 24 h before fixation, immunofluorescence staining, and 10-point DRC analysis. (B) Representative images showing ZIKV envelope antigen (green) and cell nuclei (red). Rates of infection are shown for DMSO, MPA, and selected BMZs as indicated (140 µM (**23**), 88 µM (**24**), 28 µM (**30**), 87 µM (**32**), 97 µM (**34**), 57 µM (**35**), and 18 µM (**39**)). Scale bar, 0.1 µm. (C) Representative DRCs of selected compounds and reference inhibitor MPA. Percentage ZIKV inhibition and cell viability are shown in black and red, respectively.

Structure-activity relationship (SAR) analysis

Based on different substituents at the C-2 position of the BMZ ring, BMZs **1**-**50** were classified into four categories **A**-**D** (Table 1). Structurally diverse substituents were introduced to the N-1 position of the BMZ ring, including simple benzyl, substituted benzyl (4-OMe-benzyl, 2-chloro-benzyl, and 3-pyridinylmethyl), or alkyl (3-morpholylpropyl and propyl), as well as the CF_3 group at the C-5 position. As a result, variations in the activity of compounds in each category may be attributed to different groups at these N-1 and C-5 positions.

The ZIKV screening results presented in Table 1 show that compounds in category **A** (**1**-**19**) with C-2-substituted phenyl exhibited good activity, with up to EC_{50} = 2.5 µM for the 4-hydroxy-substituted compound **4**, but had poor selectivity (SI<5).

Category **B** contains derivatives with the 4-pyridine moiety at the C-2 position, which showed good selectivity up to 16.9 (compounds **23**, **24**). Compared to compound **4**, the substitution of the vanillin moiety at the C-2 position by the 4-pyridinyl substituent (compound **23**) led to a 4.4-fold increase in SI value.

The importance of a heterocyclic moiety at the C-2 and the CF_3 group at the C-5 positions are again found in category **C** with the C-2 substituted pyrrole. The presence of these substituents led to good activity and good selectivity (SI up to 19.5) (**30**, **32**, **34**, and **35**). Without the CF_3 group, no activity was observed (**29** and **31**). It seems that the CF_3 group at the C-5 leads to a decrease in activity only when combined with an electron releasing groups at N-1 such as 4-OMe-benzyl or propyl (**25** and **28** in category **B** or **33** and **36** in category **C**).

For derivatives in category **D** bearing the naphthalenyl moieties at the C-2 position of the BMZ ring (**37**-**50**), all compounds with the CF_3 substituents at the C-5 positions (**38**, **40**, **44**, **45**, **48**, **49**, **50**) did not show any activity. The presence of the substituents such as simple benzyl (**37**, **38** and **49**) or 4-OCH_3-benzyl (**41**), or morpholylpropyl (**44**) at the N-1 position, also did not lead to any difference either. The introduction of the 2-

chlorobenzyl group at the N-1 position (**39**), however, could remarkably produce significant improvement with the EC_{50} up to 1.9 μM and SI up to 37.3. The presence of the CF_3 group at the C-5 position, however, seemed to be worse in this case (**40**). It is also noted that the change of substituents within the naphthalene moiety with the free OH group being protected as the methoxy group (**46**) led to the loss of the activity.

In summary, seven BMZs (**23**, **24**, **30**, **32**, **34**, **35**, and **39**) were identified as potent inhibitors of an African ZIKV strain (Fig. 2). It seems that the aromatic heterocyclic ring, such as pyridine or pyrrole at the C-2 position and 2-Cl-benzyl, 4-OCH_3-benzyl, or 3-pyridinylmethyl at the N-1 position, in combination with a CF_3 group at the C-5 position of the BMZ ring play essential roles in anti-ZIKV activity. Notably, the hybrid structure of BMZ and naphthalene rings, with a free OH group at the C-4 position, three methoxy groups at the C-5, C-6, and C-7 positions of the naphthalene moiety, and 2-Cl-benzyl at the N-1 position of the BMZ ring (**39**), is the novel structural feature that produces anti-ZIKV activity comparable to the positive control MPA. Thus, bioisosteric groups such as CF_3 at C-5 and Cl at N-1 substituents are necessary for enhancing anti-ZIKV activity.

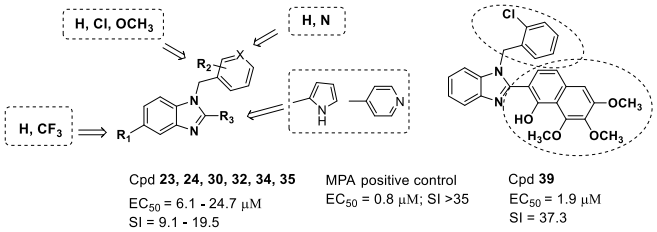

Fig. 2 Potent anti-ZIKV structures of evaluated BMZs.

Evaluation of anti-ZIKV activity in human neural stem cells

ZIKV infection can dramatically affect fetal neural development, and strong evidence indicates that neural stem cells or progenitors and neurons support ZIKV entry and RNA replication.[19] Therefore, the antiviral activity of the selected BMZs (**23**, **24**, **30**, **32**, **34**, **35**, and **39**) was tested in primary human neural stem cells, a model physiologically resembling the situation in patients. Except for **34**, all tested compounds exhibited good antiviral activity with EC_{50} at low micromolar levels. The most potent compound (**39**) showed a submicromolar EC_{50} and SI of 12.1 (Table 2).

Evaluation of cell-protective effects of BMZs in ZIKV-infected cells

As ZIKV infection induces cytopathic effects (CPEs),[20] we tested whether treatment with BMZs could prevent CPEs induced by ZIKV replication. Based on the results of our primary screen and human neural stem cell experiments, we selected four compounds for testing (**23**, **30**, **35**, and **39**). Compound **24** was in the same category as **23**. Upon pre-treatment of Vero cells with MPA, 100% of CPEs were inhibited (Fig. 3). Selected BMZs (**23**, **30**, **35**, and **39**) reduced CPEs in a dose-dependent manner. Compared with the positive control MPA, **35** at 17 μM, which is below the CC_{50} of 50 μM, showed the highest CPE inhibition.

Table 2. Validation of anti-ZIKV activity of selected BMZs in human neural stem cells.

Compound	EC_{50} (μM)[a]	CC_{50} (μM)[a]	SI[b]
23	3.0±1.4	18.2±1.3	6.1
24	3.4±1.5	17.5±1.2	5.1
30	2.2±1.3	10.4±1.1	4.7
32	4.2±1.3	32.8±1.1	7.8
34	21.0±1.3	114.5±1.1	5.4
35	4.7±2.0	28.1±1.7	5.9
39	0.6±1.5	7.3±2.2	12.1
MPA	0.02±0.003	0.5±0.07	25.0

[a]EC_{50} and CC_{50} values were calculated by 10-point DRC analysis in triplicate. Experiments were repeated at least two times independently. [b]SI = CC_{50}/EC_{50}.

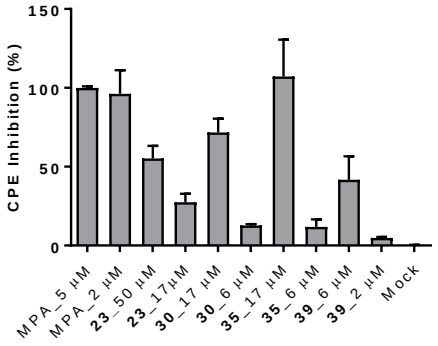

Fig. 3 BMZs protect against cytopathic effects induced by ZIKV infection. Cell protection was evaluated by assessing cell viability in ZIKV-infected Vero cells in the presence of BMZs (**23**, **30**, **35**, and **39**) and MPA at the indicated concentrations. CPE inhibition is shown as a percentage, and the positive control MPA was set to 100% inhibition of CPE.

Evaluation of antiviral activity using an Asian ZIKV strain

To assess differences in the susceptibility of viral strains to BMZs, we evaluated selected compounds using an Asian ZIKV strain. All selected BMZs showed potent antiviral activity with an average SI of ~68 and maximum SI of 115.3 (**35**) (Table 3). Notably, whereas all tested compounds exhibited remarkably improved EC_{50} against the Asian ZIKV strain as compared with the African ZIKV strain (Table 1), the EC_{50} of compound **39** remained almost the same. This could be attributed to significant phenotypic differences in the replication characteristics between African and Asian lineage ZIKV strains, leading to the observed differences in the activity of the tested compounds, especially **39**.[21]

Table 3. Validation of antiviral activity of selected BMZs using an Asian ZIKV strain.

Compound	EC_{50} (μM)[a]	CC_{50} (μM)[a]	SI[b]
23	0.2±0.2	24.4±1.3	112.0
24	0.5±0.3	29.1±1.6	58.0
30	0.5±0.1	20.7±2.5	41.4
32	0.3±0.2	20.1±3.2	67.0
34	1.3±0.4	97.4±1.6	74.9
35	0.3±0.09	34.6±2.0	115.3
39	1.5±0.1	>9.4	>6.3
MPA	0.06±0.05	>5.9	>98.3

[a]EC_{50} and CC_{50} values were calculated by 10-point DRC analysis in triplicate. Experiments were repeated at least two times independently. [b]SI = CC_{50}/EC_{50}.

Mechanism of action studies

Lastly, to determine which stage of the viral life cycle was inhibited by BMZs, we conducted a time-of-addition study with the African ZIKV MR-766, as this strain shows higher infection rates, is more virulent, and causes more severe brain damage than the current Asian lineage.[22] Cells were treated at the indicated time points with compound **39** (Fig. 4A). As controls, the nucleoside replication inhibitor MPA and NH_4Cl, an early virus entry inhibitor that blocks acidification of the late endosome and prevents fusion of the flaviviruses envelope to the endosomal membrane, were tested side-by-side. We found that MPA strongly inhibited ZIKV at all time points, whereas NH_4Cl was active predominantly at early time points (-1, 0, and 1 h; Fig. 4B, left). The inhibition pattern of compound **39** was similar to that of MPA, and passaging the viral supernatants to naive target cells confirmed these results (Fig. 4B, right). Importantly, these experiments were conducted at non-cytotoxic compound concentrations (Fig. 4C). Next, we investigated whether BMZs blocked the pre- or post-entry step in the viral life cycle (Fig. 4D). Therefore, we delivered compounds during the entire infection period (30 hours post-infection (hpi)) or removed them at 3 hpi (t = 3 h), after viral entry had occurred. NH_4Cl inhibited infection when removed at 3 hpi, whereas the inhibitory effects of compound **39** and MPA were significantly reduced when they were removed at 3 hpi (Fig. 4D, left). After transferring viral supernatants to naïve target cells, we observed similar trends in ZIKV inhibition (Fig. 4D, right). Together, these results indicate that BMZs inhibit ZIKV RNA replication.

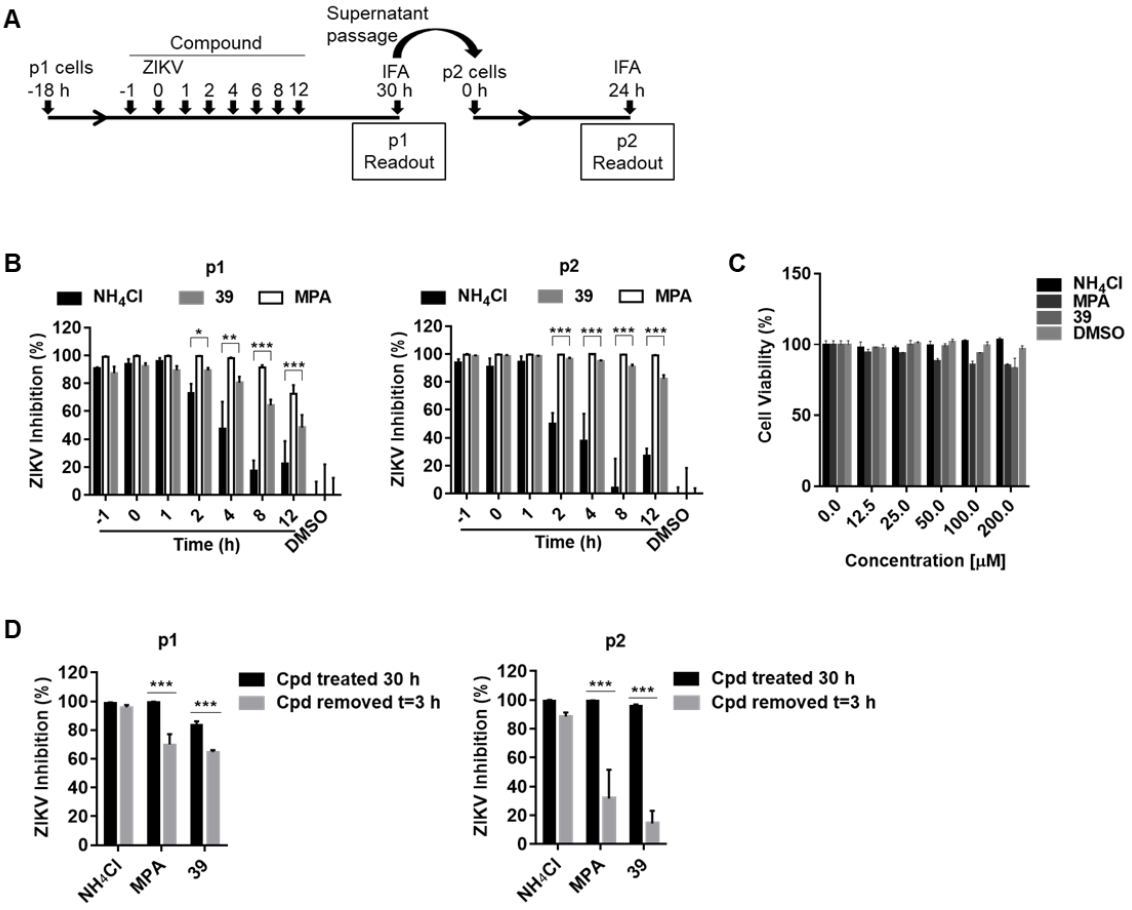

Figure 4. Time-of-addition study with ZIKV. (A) Experimental scheme. (B) Graph showing ZIKV inhibition in passage 1 (p1, left panel) and p2 (right panel) cells. As controls, NH_4Cl (2 mM, black), MPA (25 μM, white), and DMSO (0.5%) were compared with BMZ compound **39** (25 μM, gray). Compounds were added at different time points pre- or post-infection as indicated. (C) Cell viability in the presence of inhibitors was evaluated using a commercial kit. (D) ZIKV inhibition in p1 (left panel) and p2 (right panel) cells with or without drug removal. Cells were treated with the indicated drugs for 1 h before infection and incubated for 30 h (black) or removed at t = 3 h (grey). The percentage inhibition is shown for a representative experiment (n = 3). ***p <0.001, **p <0.01, or *p <0.05.

Conclusions

For the first time, we synthesized a series of 50 structurally diverse BMZ derivatives through an efficient and environmentally friendly one-pot route and screened compounds for their anti-ZIKV activity. The synthetic protocol is general, simple, fast, using inexpensive and easily available $Na_2S_2O_5$ which could be an effective method for large-scale synthesis. Seven compounds efficiently inhibited ZIKV RNA replication in different human and non-human cell lines. The aromatic heterocyclic ring at the C-2 position and 2-Cl-benzyl, 4-OCH3-benzyl, or 3-pyridinylmethyl at the N-1 position, in combination with a CF3 group at the C-5 position of the BMZ ring (**23**, **24**, **30**, **32**, **34**, **35**) play essential roles in anti-ZIKV activity. Notably, the hybrid structure of BMZ and naphthalene ring with bioisosteric groups such as CF3 at C-5 and Cl at N-1 substituents (39) is the novel structural feature that produces anti-ZIKV activity comparable to the positive control MPA. Importantly, BMZs inhibited ZIKV in human neural stem cells, which are physiologically the most relevant system, as ZIKV infection is associated with severe congenital anomalies like microcephaly. Compound **39** displayed the highest antiviral efficacy against the African ZIKV strain in terms of SI values in Huh-7 (SI>37) and neural stem cells (SI=12), whereas compound **35** possessed the highest activity against the Asian ZIKV strain (SI=115) in Vero cells. Furthermore, a time-of-addition study indicated that BMZs inhibited ZIKV RNA replication. Although further intensive compound optimization and biological studies are required, BMZs are a new chemical class for anti-ZIKV drug development, and both **35** and **39** are favorable lead compounds for further optimization as well as suitable chemical tools to study the viral life cycle.

Experimental section

General information

Reactions were monitored by thin-layer chromatography on 0.2-mm pre-coated silica gel 60 F254 plates (Merck). ^{1}H NMR and ^{13}C NMR spectra were measured with Bruker Avance 300 MHz, Bruker Avance 500 MHz, and Bruker Avance 600 MHz spectrometers. Mass spectrometry data were recorded on an 1100 series LC-MSD-Trap-LS Agilent spectrometer, and HRESI-MS observation was performed on a Bruker MicrOTOF-Q mass spectrometer. FT-IR was conducted using the KBr pellet method with a Thermo Nicolet 6700. Chemical shifts are given in parts per million relative to tetramethylsilane (Me_4Si, $\delta = 0$); J values are given in Hz.

Chemistry

General procedure for the synthesis of BMZ derivatives (1-50): A mixture of aldehyde (0.2 mmol), diamine (0.2 mmol), and $Na_2S_2O_5$ (0.6 mmol) in ethanol (1.0 mL) was stirred at 80°C for 0.5-2 h. The reaction was quenched with 5 mL saturated $NaHCO_3$ and the reaction mixture was extracted with ethyl acetate (3 × 10 mL). The combined organic layers were washed with H_2O (30 mL) and brine (30 mL) and dried over Na_2SO_4, and the solvent was evaporated under reduced pressure. Purification by column chromatography on silica gel was performed using a mixture of hexane and ethyl acetate as solvent to afford the desired BMZ products. All compounds were ≥95% pure according to high-resolution ^{1}H-NMR of 500 MHz (see spectra in Supporting Information).

Spectral data of compounds **2**-**6**, **8**, **15**, **21**, **22**, **24**, **25**, **30**, **31**, **33**, **35**,[15] **11**-**13**,[23] and **20**[24] are described in previous literature.

4-(1-Benzyl-1*H*-benzo[*d*]imidazol-2-yl)-2-methoxyphenol (1): Yield 91% as light brown solid; mp 140-142°C; IR ν_{max} (KBr): 2927, 1599, 1495, 1410, 1283, 1238, 1118, 735; ESI-MS found *m/z* 331.0 $[M+H]^+$ (calcd. 331.14, $C_{21}H_{19}N_2O_2$); ^{1}H-NMR (500 MHz, DMSO-*d6*): 9.51 (*s*, 1H), 7.69 (*d*, J = 7.0 Hz, 1H), 7.42 (*d*, J = 7.0 Hz, 1H), 7.31 (*t,* J = 7.0 Hz, 2H), 7.26-7.19 (*m*, 4H), 7.14 (*dd,* J = 2.0 Hz, J = 8.25 Hz, 1H), 7.04 (*d*, J = 7.5 Hz, 2H), 6.86 (*d*, J = 8.0 Hz, 1H), 5.57 (*s*, 2H), 3.66 (*s*, 3H); ^{13}C-NMR (125 MHz, DMSO-*d6*): 153.6, 148.2, 147.5, 142.6, 137.2, 136.1, 128.8, 127.4, 125.9, 122.3, 122.0, 121.9, 120.8, 118.9, 115.6, 112.9, 110.7, 55.4, 47.5.

2-Methoxy-4-(1-(pyridin-3-ylmethyl)-1*H*-benzo[*d*]imidazol-2-yl)phenol (7): Yield 80% as pale yellow solid; mp 149-151°C; IR (KBr) ν_{max}: 2922, 1595, 1488, 1458, 1428, 1280, 1223, 1026, 810, 743; ESI-MS *m/z* 331.9 $[M+H]^+$, 329.9 $[M+H]^-$; ^{1}H-NMR (300 MHz, $CDCl_3$): 8.57 (*d*, J = 6.9 Hz, 1H), 8.51 (*s*, 1H), 7.87 (*d*, J = 7.8 Hz, 1H), 7.20-7.37 (*m*, 6H), 7.04 (*dd,* J_1 = 8.4 Hz, J_2 = 2.4 Hz, 1H), 6.95 (*d*, J = 8.1 Hz, 1H), 6.69 (*brs*, 1H, -OH), 5.50 (*s*, 2H), 3.82 (*s*, 3H); ^{13}C-NMR (125 MHz, DMSO-*d6*): 153.6, 148.7, 148.3, 147.8, 147.6, 142.6, 135.8, 133.9, 132.8, 123.7, 122.4, 122.1, 122.0, 120.8, 119.0, 116.0, 113.0, 110.7, 55.5, 45.3.

2-Methoxy-4-(1-(3-morpholinopropyl)-1*H*-benzo[*d*]imidazol-2-yl)phenol (9): Yield 64% as **w**hite solid; mp 240–242°C; IR ν_{max} (KBr): 2951, 2914, 2850, 1596, 1498, 1465, 1312, 1271, 1176, 1119, 1032, 761; ESI-MS found *m/z* 368.1 $[M+H]^+$ (calcd. 368.19, $C_{21}H_{26}N_3O_3$); ^{1}H-NMR (500 MHz, $CDCl_3$) 7.80 (*q*, J = 3.0 Hz, 1H), 7.42 (*q*, J = 3.0 Hz, 1H), 7.32 (*d*, J = 1.5 Hz, 1H), 7.27–7.32 (*m*, 2H), 7.17 (*dd,* J = 1.5; 8.0 Hz, 1H), 7.01 (*d*, J = 8.0 Hz, 1H), 4.36 (*t*, J = 7.5 Hz, 2H), 3.95 (*s*, 3H), 3.63 (*t*, J = 4.3 Hz, 4H), 2.29 (*s*, 4H), 2.25 (*t*, J = 6.8 Hz, 2H), 1.89-1.95 (*m*, 2H); ^{13}C-NMR (125 MHz, $CDCl_3$): 153.7, 147.3, 147.0, 143.0, 135.8, 122.6, 122.5, 122.4, 122.2, 119.8, 114.5, 112.4, 110.0, 66.9, 56.2, 55.4, 53.6, 42.7, 26.6.

2-Methoxy-4-(1-(3-morpholinopropyl)-5-(trifluoromethyl)-1H-benzo[d]imidazol-2-yl)phenol (10): Yield 68% as white solid; mp 186-188°C; IR (KBr) ν_{max} cm^{-1}: 2952, 2826, 1621, 1599, 1534, 1485, 1429, 1328, 1277, 1227, 1152, 1112, 1046, 853, 817. ESI-MS found *m/z* 436.1 $[M+H]^+$ (calcd. 436.18, $C_{22}H_{25}F_3N_3O_3$); ^{1}H-NMR (500 MHz, $CDCl_3$): 8.07 (*s*, 1H, 7.51-7.55 (*m*, 2H), 7.31 (*d*, J = 2.0 Hz, 1H), 7.18 (*dd,* J = 2.0; 8.5 Hz, 1H), 7.02 (*d*, J = 8.0 Hz, 1H), 4.42 (*t*, J = 7.3 Hz, 2H), 3.95 (*s*, 3H), 3.65 (*s*, 4H), 2.29 (*q*, J = 9.5 Hz, 6H), 1.93 (*t*, J = 7.0 Hz, 2H); ^{13}C-NMR (125 MHz, $CDCl_3$): 154.6, 146.8, 146.2, 141.3, 136.7, 124.9, 123.8, 122.7, 121.1, 120.6, 118.4, 116.4, 116.3, 113.7, 111.3, 109.3, 65.6, 55.1, 54.2, 52.4, 41.8, 29.9.

1-(2-Chlorobenzyl)-2-(3-fluorophenyl)-1*H*-benzo[*d*]imidazole (14): Yield 85% as white solid; mp 163-165°C; IR(KBr) ν_{max}: 3059, 2923, 1614, 1585, 1517, 1476, 1441, 1390, 1269, 1201, 1154, 1043, 903, 793, 744, 691; HR-ESI-MS found *m/z* 337.0910 $[M+H]^+$ (calcd. 337.0908, $C_{20}H_{15}N_2ClF$)); ^{1}H-NMR (300 MHz, $CDCl_3$): 7.91 (*d*, J = 8.1 Hz, 1H), 7.50 (*dd,* J_1 = 8.1 Hz, J_2 = 1.2 Hz, 1H), 7.37-7.46 (*m*, 4H), 7.35 (*dd,* J_1 = 8.1 Hz, J_2 = 1.2 Hz, 1H), 7.31 (*d*, J = 1.2 Hz, 1H), 7.14-7.22 (*m*, 3H), 6.76 (*dd,* J_1 = 7.5 Hz, J_2 = 0.9 Hz, 1H), 5.52 (*s*, 2H); ^{13}C-NMR (125 MHz, DMSO-*d6*): 162.9, 160.9, 151.92, 151.90, 142.4, 135.9, 133.8, 132.2, 132.1, 131.3, 130.93, 130.87, 129.6, 129.4, 127.7,127.3, 124.89, 124.87, 124.9, 123.2, 122.5, 119.5, 116.9, 116.7 115.8, 115.6, 110.9, 45.7.

2-(3-Fluorophenyl)-1-(3-morpholinopropyl)-1*H*-benzo[*d*]imidazole (16): Yield 75% as white solid; mp 60-62°C; IR (KBr) ν_{max}: 3375, 2952, 2849, 2814, 1616, 1587, 1451, 1325, 1279, 1140, 1114, 917, 791, 747; ESI-MS found *m/z* 340.0 $[M+H]^+$ (calcd. 340.18, $C_{20}H_{23}FN_3O$); ^{1}H-NMR (500 MHz, $CDCl_3$) δ 7.81-7.84 (*m*, 1H), 7.53 (*d*, J = 8.0 Hz, 1H), 7.44 – 7.51 (*m*, 3H), 7.29-7.33 (*m*, 2H), 7.19-7.23 (*m*, 1H), 4.38 (*t*, J = 7.3 Hz, 2H), 3.61 (*t*, J = 4.8 Hz, 4H), 2.28 (*s*, 4H), 2.23 (*t*, J = 6.8 Hz, 2H), 1.89-1.95 (*m*, 2H); ^{13}C-NMR (125 MHz, $CDCl_3$) δ 163.7 (161.7), 152.2, 143.0, 135.7, 132.8 (132.7), 130.5 (130.4), 125.1 (125.0), 123.1, 122.6, 120.1, 116.8 (116.7), 116.5 (116.4), 110.2, 66.8, 55.1, 53.5, 42.6, 26.4.

5-(Trifluoromethyl)-2-(3-fluorophenyl)-1-(3-morpholinopropyl)-1*H*-benzo[*d*]imidazole (17): Yield 70% as white solid; mp 120-122°C; IR

(KBr) ν_{max}: 3066, 2957, 2859, 2807, 1615, 1589, 1436, 1331, 1264, 1224, 1151, 1113, 1049, 883, 860, 822, 786. ESI-MS found *m/z* 408.0 $[M+H]^+$ (calcd. 408.17, $C_{21}H_{22}F_4N_3O$); ^{1}H-NMR (500 MHz, $CDCl_3$) 8.09 (*s*, 1H), 7.52 – 7.58 (*m*, 4H), 7.49 (*q*, J = 4.7 Hz, 1H), 7.23-7.27 (*m*, 1H), 4.43 (*t*, J = 7.3 Hz, 2H), 3.61 (*t*, J = 4.0 Hz, 4H), 2.28 (*s*, 4H), 2.44 (*t*, J = 4.5 Hz, 2H), 1.89-1.95 (*m*, 2H); ^{13}C-NMR (125 MHz, $CDCl_3$) 163.7 (161.8), 154.1 (154.0), 142.5, 137.7, 132.1 (132.0), 130.7 (130.6), 125.1 (125.0), 125.9 (125.3, 124.8), 123.7, 119.89 (119.86, 119.83), 117.89 (117.86, 117.83), 116.6 (116.4), 110.7, 66.7, 55.0, 53.5, 42.8, 26.3.

2-(2,4-dimethoxyphenyl)-1-(3-morpholinopropyl)-1*H*-benzo[*d*]imidazole (18): Yield 72% as **y**ellow solid; mp 92-94°C; IR (KBr) ν_{max}: 3054, 2953, 2850, 2811, 1614, 1580, 1534, 1457, 1388, 1279, 1209, 1160, 1116, 1030, 833, 747; ESI-MS found *m/z* 382.1 $[M+H]^+$ (calcd. 382.21, $C_{22}H_{28}N_3O_3$); ^{1}H-NMR (500 MHz, DMSO) 7.61 (*d*, J = 8.0 Hz, 1H), 7.59 (*d*, J = 8.0 Hz, 1H), 7.34 (*d*, J = 8.5 Hz, 1H), 7.24 (*t*, J = 7.5 Hz, 1H), 7.19 (*t*, J = 7.5 Hz, 1H), 6.75 (*d*, J = 2.0 Hz, 1H), 6.68 (*dd,* J = 3.0; 8.5 Hz, 1H), 4.07 (*t*, J = 7.3 Hz, 2H), 3.85 (*s*, 3H), 3.78 (*s*, 3H), 3.41 (*t*, J = 4.0 Hz, 4H), 2.09 (*m*, 6H), 1.64-1.69 (*m*, 2H); ^{13}C-NMR (125 MHz, DMSO) 162.1, 158.3, 151.2, 142.8, 135.0, 132.6, 121.9, 121.3, 118.9, 112.2, 110.4, 105.4, 98.5, 66.1, 55.6, 55.5, 54.7, 52.9, 41.5, 25.7.

5-(Trifluoromethyl)-2-(2,4-dimethoxyphenyl)-1-(3-morpholinopropyl)-1*H*- benzo[*d*]imidazole (19): Yield 64% as yellow solid; mp 112-114°C; IR (KBr) ν_{max}: 2947, 2815, 1616, 1578, 1536, 1466, 1436, 1330, 1211, 1158, 1117, 1029, 880, 844, 803. ESI-MS found *m/z* 450.1 $[M+H]^+$ (calcd. 450.20, $C_{23}H_{27}F_3N_3O_3$); ^{1}H-NMR (500 MHz, $CDCl_3$) 8.07 (*br*, 1H), 7.52 (*brs*, 2H), 7.41 (*d*, J = 8.5 Hz, 1H), 7.26 (*s*, 1H), 6.62 (*dd,* J = 2.0; 8.5 Hz, 1H), 6.58 (*d*, J = 8.0 Hz, 1H), 4.18 (*t*, J = 7.8 Hz, 2H), 3.88 (*s*, 3H), 3.79 (*s*, 3H), 3.60 (*t*, J = 4.5 Hz, 4H), 2.23 (*s*, 4H), 2.18 (*q*, J = 5.2 Hz, 2H), 1.80 (*t*, J = 7.0, 2H); ^{13}C-NMR (125 MHz, $CDCl_3$) 162.8, 158.6, 153.8, 142.7, 137.3, 132.8, 126.0, 124.5 (124.2, 123.9), 119.2 (119.1), 117.5 (117.4), 112.0, 110.2, 105.2, 98.8, 66.8, 55.7, 55.6, 55.2, 53.4, 42.4, 26.1.

1-(2-Chlorobenzyl)-2-(pyridin-4-yl)-5-(trifluoromethyl)-1*H*-benzo[*d*]imidazole (23): Yield 80% as pale yellow solid; mp 150-152°C; IR (KBr) ν_{max}:3057, 2962, 2928, 1600, 1473, 1443, 1386, 1326, 1162, 1109, 1044, 923, 811, 756, 695, 659; HR-ESI-MS found *m/z* 388.0835 $[M+H]^+$ (calcd. 388.0828, $C_{20}H_{14}N_3ClF_3$); ^{1}H-NMR (300 MHz, $CDCl_3$): 8.75 (*d*, J = 5.1 Hz, 2H), 8.20 (*s*, 1H), 7.58 (*dd,* J_1 = 4.5 Hz, J_2 = 1.8 Hz, 2H), 7.54 (*dd,* J_1 = 4.8 Hz, J_2 = 1.2 Hz, 1H), 7.50 (*d*, J = 0.9 Hz, 1H), 7.31-7.35 (*m*, 2H), 7.19 (*td,* J_1 = 7.8 Hz, J_2 = 1.2 Hz, 1H), 6.68 (*d*, J = 7.8 Hz, 1H), 5.58 (*s*, 2H); ^{13}C-NMR (125 MHz, DMSO-*d6*): 153.2, 150.2, 141.9, 138.3, 136.8, 133.2, 131.5, 129.7, 129.6, 127.8, 127.6, 125.9, 123.8, 123.5, 123.0, 120.1, 117.24, 117.21, 112.4, 54.8.

1-(Pyridin-3-ylmethyl)-2-(pyridin-4-yl)-1*H*-benzo[*d*]imidazole (26): Yield 83% as brownish yellow wax; IR (KBr) ν_{max}: 2923, 2852, 1600, 1458, 1416, 1392, 1331, 1317, 821, 771, 758, 670; HR-ESI-MS found *m/z* 287.1289 $[M+H]^+$ (calcd. 287.1297, $C_{18}H_{15}N_4$); ^{1}H-NMR (300 MHz, $CDCl_3$): 8.75 (*d*, J = 5.4 Hz, 2H), 8.59 (*d*, J = 4.2 Hz, 1H), 8.50 (*s*, 1H), 7.91 (*d*, J = 7.2 Hz, 1H), 7.59 (*dd,* J_1 = 4.5 Hz, J_2 = 1.5 Hz, 2H), 7.25-7.40 (*m*, 5H), 5.53 (*s*, 2H); ^{13}C-NMR (125 MHz, DMSO-*d6*): 150.5, 150.2, 142.5, 137.5, 136.6, 136.2, 128.8, 127.5, 126.0, 123.4, 123.1, 122.6, 119.7, 111.3, 47.5.

1-(Pyridin-3-ylmethyl)-2-(pyridin-4-yl)-5-(trifluoromethyl)-1*H*-benzo[*d*]imidazole (27): Yield 88% as white solid; mp 128-130°C; IR (KBr) ν_{max}: 3372, 3048, 2922, 1602, 1436, 1412, 1325, 1233, 1167, 1117, 1048, 839, 814, 706; ESI-MS *m/z* 355.0 $[M+H]^+$ (calcd. 355.12, $C_{19}H_{14}F_3N_4$); ^{1}H-NMR (500 MHz, DMSO-*d6*)*:* 8.77 (*d*, J = 5.0 Hz, 2H, 8.45 (*d*, J = 4.0 Hz, 1H, 8.32 (*s*, 1H, 8.18 (*s*, 1H, 7.87 (*d*, J = 8.5 Hz, 1H, 7.77 (*d*, J = 5.5 Hz, 2H, 7.66 (*d*, J = 8.5 Hz, 1H, 7.32 (*d*, J = 8.0 Hz, 1H, 7.28 (*t,* J = 8.0 Hz, 1H, 5.80 (*s*, 2H); ^{13}C-NMR (125 MHz, DMSO-*d6*): 152.9; 150.3; 149.0; 147.8; 141.9; 138.2; 136.7; 134.0; 131.8; 123.8; 123.6; 123.3; 120.1; 117.2; 112.5; 45.6.

1-Propyl-2-(pyridin-4-yl)-5-(trifluoromethyl)-1*H*-benzo[*d*]imidazole (28): Yield 87% as white solid; mp 110-112°C; IR (KBr) ν_{max}: 2960; 2880; 1604; 1472; 1335; 1148; 1120; 864; 836; 804. ESI-MS found *m/z* 306.0 (calcd. 306.12, $C_{16}H_{15}F_3N_3$); ^{1}H-NMR (500 MHz, DMSO-*d6*)*:* 8.82 (*dd,* J = 4.5 Hz, 2H, 8.11 (*s*, 1H, 7.98 (*d*, J = 8.5 Hz, 1H, 7.82 (*d*, J = 4.5, 2H, 7.66 (*d*, J = 8.5, 1H, 4.39 (*t,* J = 7.5, 2H, 1.70 (*d*, J = 15, 2H, 0.74 (*t,* J = 7.0, 3H); ^{13}C-NMR (125 MHz, DMSO-*d6*): 152.7; 150.3; 141.8; 138.1; 137.3; 123.8; 123.4; 123.2; 119.6; 117.0; 112.4; 45.9; 22.6; 10.7.

1-Benzyl-2-(1*H*-pyrrol-2-yl)-1*H*-benzo[*d*]imidazole (29): Yield 92% as white solid; mp 149-151°C; IR (KBr) ν_{max}: 3414, 3057, 2923, 2856, 1601, 1577, 1497, 1453, 1392, 1356, 1135, 927, 731; HR-ESI-MS found *m/z* 274.1341 $[M+H]^+$ (calcd. 274.1344, $C_{18}H_{16}N_3$); ^{1}H-NMR (500 MHz, DMSO-*d6*): 7.64 (*d*, J = 8.0 Hz, 1H), 7.48 (*d*, J = 8.0 Hz, 1H), 7.32 (*t,* J = 7.5 Hz, 2H), 7.16-7.26 (*m*, 3H), 7.08 (*d*, J = 7.5 Hz, 2H), 6.97 (*s*, 1H), 6.49 (*s*, 1H), 6.15 (*d*, J = 3Hz, 1H), 5.71 (*s*, 2H); ^{13}C-NMR (125 MHz, DMSO-*d6*): 147.1, 142.5, 137.0, 136.1, 128.7, 127.3, 126.0, 122.0, 121.9, 121.6, 120.7, 118.1, 110.1, 109.8, 109.3, 47.0.

1-(4-Methoxybenzyl)-2-(1*H*-pyrrol-2-yl)-1*H*-benzo[*d*]imidazole (32): Yield 87% as white solid; mp 123-125°C; IR (KBr) ν_{max}: 3278, 2923, 2854, 1655, 1447, 1405, 1312, 1137, 1088, 1040, 759; HR-ESI-MS found *m/z* 304.1444 $[M+H]^+$ (calcd. 304.1450, $C_{19}H_{18}N_3O$); ^{1}H-NMR (300 MHz, $CDCl_3$): 11.02 (*s*, 1H), 7.75 (*dd,* J_1 = 6.3 Hz, J_2 = 0.9 Hz, 1H), 7.18-7.30 (*m*, 3H), 7.11 (*d*, J = 8.7 Hz, 2H), 7.04 (*d*, J = 1.2 Hz, 1H), 6.87 (*d*, J = 8.4 Hz, 2H), 6.54 (*m*, 1H), 6.28 (*m*, 1H), 5.58 (*s*, 2H); ^{13}C-NMR (125 MHz, DMSO-*d6*): 158.5, 147.0, 142.6, 136.0, 128.7, 127.3, 121.9, 121.8, 121.5, 120.8, 118.1, 114.2, 110.2, 109.8, 109.3, 55.0, 46.5.

1-(Pyridine-3-ylmethyl)-2-pyrrolyl-1*H*-benzo[*d*]imidazole (34): Yield 87% as white solid; mp 189-191°C; IR (KBr) ν_{max}: 3433, 3172, 2924, 2854, 1736, 1617, 1577, 1500, 1456, 1401, 1131, 1028, 829, 746, 708; HR-ESI-MS found *m/z* 275.1293 $[M+H]^+$ (calcd. 275.1297, $C_{17}H_{15}N_4$); ^{1}H-NMR (500 MHz, DMSO-*d6*): 11.87 (*s*, 1H, N-H), 8.46 (*dd,* J_1 = 4.5 Hz, J_2 = 1.5 Hz, 1H), 8.40 (*d*, *J* = 1.5 Hz, 1H), 7.66 (*dd,* J_1 = 7.0 Hz, J_2 = 1.0 Hz, 1H), 7.55 (*dd,* J_1 = 7.0 Hz, J_2 = 1.5 Hz, 1H), 7.37 (td, J_1 = 8.0 Hz, J_2 = 2.0 Hz, 1H),7.31-7.33 (*m*, 1H), 7.18-7.25 (2H), 6.97 (*m*, 1H), 6.55-6.57 (*m*, 1H), 6.17-6.19 (*m*, 1H), 5.78 (*s*, 2H); ^{13}C-NMR (125 MHz, DMSO-*d6*): 148.6, 147.7, 146.9, 142.5, 135.8, 133.8, 132.6, 123.8, 122.2, 111.0, 121.7, 118.2, 110.1, 109.8, 109.4, 44.8.

1-Propyl-2-(1*H*-pyrrol-2-yl)-5-(trifluoromethyl)-1*H*-benzimidazole (36): Yield 78% as white solid; mp 109-111°C; IR (KBr) ν_{max}: 3132; 2974; 2874; 1624; 1589; 1500; 1330; 1234; 1149; 1111; 924; 810; 729; ESI-MS *m/z* 294.0 $[M+H]^+$; ^{1}H-NMR (500 MHz, DMSO-*d6*): 11.90 (*s*, 1H), 7.88 (*s*, 1H), 7.82 (*d*, J = 8.5, 1H), 7.52 (*dd,* J = 8.5, 1H), 7.04 (*t,* J = 1.75, 1H), 6.79 (*d*, J = 4.5, 1H), 6.30 (*d*, J = 6, 1H), 4.44 (*t,* J = 7.5, 2H), 1.81 (*d*, J = 14.5, 2H), 0.93 (*t,* J = 7.5, 3H); ^{13}C-NMR (125 MHz, DMSO-*d6*, δ *ppm*): 148.8, 141.9, 138.3, 122.8, 122.5, 122.2, 120.3, 118.2, 114.9, 111.1, 110.5, 109.8, 45.4, 22.4, 10.9.

3-(1-Benzyl-1*H*-benzo[*d*]imidazol-2-yl)-6,7,8-trimethoxynaphthalen-1-ol (37): Yield 81% as pale yellow solid; mp 94-96°C; IR (KBr) ν_{max}: 3346; 2931; 1722, 1612; 1453; 1352; 1253; 1106; 1024; 731; ESI-MS found *m/z* 441.0 $[M+H]^+$ (calcd. 441.18, $C_{27}H_{25}N_2O_4$); ^{1}H-NMR (500 MHz, DMSO-*d6*, *δ* ppm)*:* 9.64 (1H, *s*, -OH, 7.72 (1H, *d*, J = 7 Hz, 6.51 (1H, *s*, 7.47 (1H, *d*, J = 7.5 Hz, 7.22-7.30 (5H, *m*, 7.18 (1H, *s*, 7.03-7.04 (3H, *m*), 5.68 (2H, *s*, -CH_2-, 4.00 (3H, *s*, -OMe, 3.91 (3H, *s*, -OMe, 3.87 (3H, *s,* -OMe); ^{13}C-NMR (125 MHz, DMSO-*d6*, *δ* ppm): 153.5; 153.13; 153.12; 148.1; 142.7; 141.0; 137.0; 135.9; 132.2; 128.7; 127.8; 127.4; 126.2; 122.6; 122.2; 119.2; 118.7; 113.7; 111.1; 108.3; 104.2; 62.2; 60.8; 55.7; 47.6.

3-(1-Benzyl-5-(trifluoromethyl)-1*H*-benzo[*d*]imidazol-2-yl)-6,7,8-trimethoxynaphthalen-1-ol (38): Yield 80% as pale yellow solid; mp 130-132°C; IR (KBr) ν_{max} : 3302, 2948, 1616, 1491, 1470, 1331, 1261, 1157, 1104, 1026, 888, 806, 728; ESI-MS found *m/z* 509.0 $[M+H]^+$ (calcd. 509.17, $C_{28}H_{24}F_3N_2O_4$); ^{1}H-NMR (500 MHz, DMSO-*d6*, δ ppm): 8,10 (1H, *s*, 7,72 (1H, *d*, J = 8,5 Hz, 7,68 (1H, *d*, J = 1,5 Hz, 7,58 (1H, *dd*, J_1 = 8,5 Hz, J_2 = 1,5 Hz), 7,28-7,31 (2H, *m*, 7,23-7,25 (1H, *m*, 7,20 (1H, s, 7,02-7,04 (3H, *m*, 5,74 (2H, *s*, 3,98 (3H, *s*, 3,91 (3H, *s*) ; 3,86 (3H, *s*); ^{13}C-NMR (125 MHz,

DMSO-*d6*, δ ppm): 155,5; 153,6; 153,2; 148,2; 142,1; 141,3; 138,3; 136,5; 132,2; 128,8; 127,6; 127,1; 126,2; 123,9; 123,4; 119,3; 119,0; 116,6; 114,0; 112,3; 108,1; 104,3; 62,3; 60,8; 55,8; 47,9.

3-(1-(2-Chlorobenzyl)-1*H*-benzo[*d*]imidazol-2-yl)-6,7,8-trimethoxynaphthalen-1-ol (39): Yield 85% as pale yellow solid; mp 140-142°C; IR (KBr) ν_{max}: 3307, 2929, 1615, 1575, 1457, 1263, 749; HR-ESI-MS found *m/z* 475.1425 $[M+H]^+$ (calcd. 475.1425 $C_{27}H_{24}ClN_2O$); ^{1}H-NMR (500 MHz, DMSO-*d6*, *δ* ppm): 9.67 (*s*, 1H), 7.76 (*d*, J = 7.5 Hz, 1H), 7.57 (*d*, J = 1.0 Hz, 1H), 7.51 (*d*, J = 8.0 Hz, 1H), 7.41 (*d*, J = 8.0, 1H), 7.32-7.21 (*m*, 4H), 7.14 (*s*, 1H), 6.95 (*d*, J = 1.5 Hz, 1H), 6.63 (*d*, J = 7.5 Hz, 1H), 5.70 (*s*, 2H), 3.98 (*s*, 3H), 3.90 (*s*, 3H), 3.85 (*s*, 3H); ^{13}C-NMR (125 MHz, DMSO-*d6*, *δ* ppm): 153.5, 153.3, 153.2, 148.1, 142.7, 141.1, 135.9, 134.1, 132.1, 131.4, 129.6, 129.3, 127.7, 127.6, 127.3, 122.9, 122.4, 119.3, 118.6, 113.7, 110.8, 108.0, 104.1, 62.2, 60.8, 55.7, 45.8.

3-(1-(2-Chlorobenzyl)-5-(trifluoromethyl)-1*H*-benzo[*d*]imidazol-2-yl)-6,7,8- trimethoxynaphthalen-1-ol (40): Yield 80% as pale yellow solid; mp 185-187°C; IR (KBr) ν_{max}: 3301, 2939, 1624, 1577, 1480, 1446, 1334, 1110, 748; ESI-MS found *m/z* 543.0 $[M+H]^+$ (calcd. 543.13, $C_{28}H_{23}ClF_3N_2O_4$); ^{1}H-NMR (500 MHz, DMSO-*d6*): 9.71 (*s*, 1H), 8.13 (*s*, 1H), 7.66 (*d*, J = 8.5 Hz, 1H), 7.60-7.57 (*m*, 2H), 7.52 (*d*, J = 8.0 Hz, 1H), 7.33 (*t*, J = 7.8 Hz, 1H), 7.24 (*t*, J = 7.8 Hz, 1H), 7.16 (*s*, 1H), 6.96 (*d*, J = 1.0 Hz, 1H), 6.68 (*d*, J = 7.5 Hz, 1H), 5.77 (*s*, 2H), 3.98 (*s*, 3H), 3.90 (*s*, 3H), 3.85 (*s*, 3H); ^{13}C-NMR (125 MHz, DMSO-*d6*): 155.6, 153.6, 153.2, 148.2, 142.1, 141.3, 138.3, 133.6, 132.1, 131.4, 129.7, 129.5, 127.8, 127.4, 126.9, 119.5, 118.9, 116.7, 113.9, 112.0, 107.9, 104.2, 62.2, 60.8, 55.8, 47.8.

6,7,8-Trimethoxy-3-(1-(4-methoxybenzyl)-1*H*-benzo[*d*]imidazol-2-yl)naphthalen-1-ol (41): Yield 82% as pale yellow solid; mp 93-95°C; IR (KBr) ν_{max}: 3295, 2933, 1631, 1613, 1513, 1460, 1349, 1253, 1177, 1112, 1027, 907, 821, 741; ESI-MS found *m/z* 471.0 $[M+H]^+$ (calcd. 471.19, $C_{28}H_{27}N_2O_5$); ^{1}H-NMR (500 MHz, DMSO-*d6*): 9.69 (*s*, 1H, -OH), 7.70-7.72 (*m*, 1H), 7.67 (*d*, J = 1.5 Hz, 1H), 7.48-7.50 (*m*, 1H), 7.21-7.25 (*m*, 3H), 7.05 (*d*, J = 1.5 Hz, 1H), 6.97 (*d*, J = 8.5 Hz, 2H), 6.83 (*d*, J = 8.5 Hz, 2H), 5.59 (*s*, 2H), 4.00 (*s*, 3H), 3.92 (*s*, 3H), 3.856 (*s*, 3H), 3.67 (*s*, 3H); ^{13}C-NMR (125 MHz, DMSO-*d6*): 158.5, 153.5, 153.1, 153.0, 148.1, 142.7, 141.0, 135.8, 132.2, 128.8, 127.9, 127.6, 122.5, 122.1, 119.1, 118.7, 114.1, 113.7, 111.2, 108.3, 104.2, 62.2, 60.8, 55.7, 55.0, 47.0.

6,7,8-Trimethoxy-3-(1-(pyridin-3-ylmethyl)-1*H*-benzo[*d*]imidazol-2-yl)naphthalen-1-ol (42): Yield 85% as pale yellow solid; mp 129-131°C; IR (KBr) ν_{max}: 3352, 2999, 2932, 1604, 1572, 1386, 1317, 1253, 1119, 1022, 869; 746; ESI-MS found *m/z* 442.0 $[M+H]^+$ (calcd. 442.18, $C_{26}H_{24}N_3O_4$); ^{1}H-NMR (500 MHz, DMSO-*d6*): 9.69 (1H, *s*, -OH), 8.43 (1H, *d*, J = 7 Hz), 8.30 (1H, *s*), 7.73 (1H, *m*), 7.47 (1H, *s*), 7.55 (1H, *m*), 7.35 (1H, *d*, J = 8 Hz), 7.26-7.30 (3H, *m*), 7.23 (1H, *s*), 7.03 (1H, *s*), 5.73 (2H, *s*), 4.00 (3H, *s*), 3.92 (3H, *s*), 3.87 (3H, *s*, -OMe); ^{13}C-NMR (125 MHz, DMSO-*d6*): 153.6, 153.14, 153.10, 148.8, 148.2, 147.8, 142.7, 141.1, 135.7, 134.1, 132.6, 132.2, 127.7, 123.7, 122.8, 122.3, 119.3, 118.7, 113.8, 111.0, 108.2, 104.2, 62.2, 60.8, 55.7, 45.3.

3-(1-Benzyl-5-methoxy-1*H*-benzo[*d*]imidazol-2-yl)-6,7,8-trimethoxynaphthalen-1-ol (43): Yield 81% as pale yellow solid; mp 110-112°C; IR (KBr) ν_{max}: 3354; 2923; 2852; 1618; 1486; 1382; 1266; 11123; 1027; 817. ESI-MS found *m/z* 471.1 $[M+H]^+$ (calcd. 471.19, $C_{28}H_{27}N_2O_5$); ^{1}H-NMR (500 MHz, DMSO-*d6*): 9.71 (*s*, 1H, -OH), 7.62 (*s*, 1H), 7.33 (*d*, J = 9.0 Hz, 1H), 7.22-7.28 (*m*, 4H), 7.12 (*s*, 1H), 6.99-7.02 (*m*, 3H), 6.86 (*dd*, J_1 = 8.5 Hz, J_2 = 1.2 Hz, 1H), 5.6 (*s*, 2H), 3.97 (*s*, 3H), 3.89 (*s*, 3H), 3.84 (*s*, 3H), 3.79 (*s*, 3H); ^{13}C-NMR (125 MHz, DMSO-*d6*): 156.1, 153.6, 153.5, 153.3, 148.3, 143.6, 141.5, 137.2, 132.3, 130.6, 128.9, 127.7, 126.3, 118.8, 114.5, 113.8, 112.5, 111.7, 108.4, 104.4, 101.9, 62.4, 61.0, 55.9, 55.7, 47.8.

3-(5-(Trifluoromethyl)-1-(3-morpholinopropyl)-1*H*-benzo[*d*]imidazol-2-yl)-6,7,8-trimethoxynaphthalen-1-ol (44): Yield 68% as yellowish brown solid; mp 78-80°C; IR (KBr) ν_{max}: 3353, 2940, 2853, 2816, 1616, 1578, 1472, 1331, 1256, 1155, 1111, 1024, 919, 883, 868, 808. ESI-MS found *m/z* 546.1 $[M+H]^+$ (calcd. 546.22, $C_{28}H_{31}F_3N_3O_5$); ^{1}H-NMR (500 MHz, $CDCl_3$) *δ* 9.60 (*s*, 1H, -OH), 8.11 (*brs*, 1H), 7.61 (*d*, J = 1.5 Hz, 1H), 7.55 (*brs*, 2H) 7.03 (*d*, J = 1.5 Hz, 1H), 7.00 (*s*, 1H), 4.48 (*t*, J = 7.3 Hz, 2H), 4.20 (*s*, 3H), 3.98 (*d*, J = 3.0 Hz, 6H), 3.54 (*t*, J = 4.5 Hz, 4H), 2.23 (*t*, J = 7.0 Hz, 6H), 1.88-194 (*m*, 2H); ^{13}C-NMR (125 MHz, $CDCl_3$) *δ* 150.8, 149.5, 148.9, 143.4, 137.8, 136.1, 133.1, 127.6, 123.6, 120.0, 114.8, 112.9, 108.6, 105.7, 103.5, 99.2, 62.0, 57.7, 56.6, 51.2, 50.3, 48.7, 38.1, 21.6.

1-Benzyl-5-(trifluoromethyl)-2-(4,6,7-trimethoxynaphthalen-2-yl)-1*H*-benzo[*d*]imidazole (45): Yield 71% as white wax; IR (KBr) ν_{max}: 2936, 2834, 1610, 1503, 1436, 1329, 1261, 1221, 1160, 1115, 1049, 1013, 929, 809, 732. ESI-MS found *m/z*: 493.1 $[M+H]^+$ (calcd. 493.17, $C_{28}H_{24}F_3N_2O_3$); ^{1}H-NMR (500 MHz, DMSO-*d6*, δ ppm): 8.11 (*s*, 1H), 7.81 (*s*, 1H), 7.76 (*d*, J = 8.5 Hz, 1H), 7.59 (*t*, J = 9.5 Hz, 1H), 7.44 (*s*, 1H, =CH-), 7.36 (*s*, 1H), 7.31 (*t*, J = 14.5 Hz, 2H), 7.25 (*t*, J = 14.5 Hz, 1H), 7.06 (*d*, J = 7.5 Hz, 3H), 5.76 (*s*, 2H), 3.90 (*s*, 3H), 3.89 (*s*, 3H), 3.83 (*s*, 3H); ^{13}C-NMR (125 MHz, DMSO-*d6*, δ ppm): 156.2, 154.0, 150.2, 150.1, 142.1, 138.5, 136.8, 129.4, 128.9, 127.6, 126.2, 126.1, 125.0, 123.9, 123.3, 123.1, 120.6, 120.3, 119.3, 116.5, 112.1, 107.3, 103.2, 100.0, 55.5, 55.5, 55.430. 48.0.

1-(2-Chlorobenzyl)-2-(4,6,7-trimethoxynaphthalen-2-yl)-1*H*-benzo[*d*]imidazole (46): Yield 71% as pale yellow wax; IR (KBr) ν_{max}: 3006, 2929, 2829, 1609, 1504, 1480, 1450, 1260, 1218, 1162, 1009, 850, 746, ESI-MS found *m/z*: 459.0 $[M+H]^+$) (calcd. 459.15, $C_{27}H_{24}ClN_2O_3$); ^{1}H-NMR (500 MHz, DMSO-*d6*): 7.78 (*t*, J = 8.5 Hz), 7.71 (*s*, 1H), 7.53 (*t*, J = 9 Hz, 1H), 7.47 (*t*, J = 8 Hz, 1H), 7.42 (*s*, 1H), 7.29 (*m*, 5H), 6.97 (*d*, J = 1.5 Hz, 1H), 6.71 (*d*, J = 6.5 Hz, 1H), 5.70 (*s*, 2H), 3.89 (*s*, 3H), 3.88 (*s*, 3H), 3.78 (*s*, 3H)); ^{13}C-NMR (125 MHz, DMSO-*d6*): 153.9, 153.8, 150.2, 149.9, 142.7, 136.2, 134.4, 131.3, 129.7, 129.4, 129.4, 127.8, 127.3, 125.5, 122.9, 122.4, 120.3, 120.0, 119.3, 110.7, 107.2, 102.9, 100.4, 55.5, 55.5, 55.2, 45.97.

1-(Pyridin-3-ylmethyl)-2-(4,6,7-trimethoxynaphthalen-2-yl)-1*H*-benzo[*d*]imidazole (47): Yield 82% as organe solid; mp 194-196°C; IR (KBr) ν_{max}: 2926, 2854, 1612, 1580, 1512, 1455, 1369, 1257, 1212, 1160, 1009, 739, ESI-MS found *m/z* 426.0 $[M+H]^+$) (calcd. 426.18, $C_{26}H_{24}N_3O_3$); ^{1}H-NMR (500 MHz, DMSO-*d6*): 8.43 (*t*, J = 6 Hz, 1H), 8.33 (*d*, J = 1.5 Hz, 1H), 7.79 (*s*, 1H), 7.75 (*m*, 1H), 7.59 (*m*, 1H), 7.45 (*s*, 1H), 7.37 (*t*, J = 12 Hz, 2H), 7.28 (*m*, 3H), 7.09 (*d*, J = 1 Hz, 1H), 5.76 (*s*, 2H), 3.91 (*s*, 3H), 3.90 (*s*, 3H), 3.89 (*s*, 3H,); ^{13}C-NMR (125 MHz, DMSO-*d6*): 153.9, 153.7, 150.1, 149.9, 148.7, 147.9, 142.7, 135.9, 134.1, 132.8, 129.4, 125.7, 123.7, 122.71, 122.3, 120.4, 119.9, 119.2, 110.9, 107.3, 103.4, 100.4, 55.5, 55.5, 55.4, 45.4.

1-(Pyridin-3-ylmethyl)-5-(trifluoromethyl)-2-(4,6,7-trimethoxynaphthalen-2-yl)-1*H*-benzo[*d*]imidazole (48): Yield 73% as white wax; IR (KBr) ν_{max}: 494.0 2926, 2954, 1739, 1615, 1513, 1436, 1327, 1261, 1215, 1161, 1108, 1011, 925, 813, ESI-MS found *m/z* $[M+H]^+$ (calcd. 494.17, $C_{27}H_{23}F_3N_3O_3$); ^{1}H-NMR (500 MHz, DMSO-*d6*): 8.44 (*t*, J = 6 Hz, 1H), 8.34 (*d*, J = 2 Hz, 1H, 8.12 (*s*, 1H), 7.84 (*t*, J = 14 Hz, 2H), 7.62 (*t*, J = 9.5 Hz, 1H), 7.46 (*s*, 1H), 7.40 (*s*, 1H), 7.36 (*t*, J = 7.5 Hz, 1H), 7.29 (*t*, J = 13 Hz, 1H), 7.10 (*d*, J = 1 Hz, 1H), 5.83 (*s*, 2H), 3.91 (*s*, 3H), 3.90 (*s*, 6H); ^{13}C-NMR (125 MHz, DMSO-*d6*): 156.08, 154.00, 150.17, 150.06, 148.85, 147.87, 142.13, 138.22, 134.09, 132.32, 129.35, 124.92, 123.79, 120.60, 120.24, 119.37, 116.55, 112.02, 107.35, 103.17, 100.38, 55.52, 55.48, 55.45. 45.69.

3-(1-Benzyl-5-(trifluoromethyl)-1*H*-benzo[*d*]imidazol-2-yl)-5,8-dimethoxynaphthalen-1-ol (49): Yield 79% as white solid; mp 173-175°C; IR (KBr) ν_{max}: 3425, 2938, 1619, 1506, 1455, 1397, 1329, 1255, 1154, 1103, 1047, 932, 803, 725, HR-ESI-MS found *m/z* 479.1585 $[M+H]^+$ (calcd. 479.1583, $C_{27}H_{22}N_2O_3F_3$)); ^{1}H-NMR (300 MHz, $CDCl_3$): 9.57 (*s*, 1H, OH), 8.19 (*s*, 1H), 8.05 (*d*, J = 1.5 Hz, 1H), 7.50 (*d*, J = 8.4 Hz, 1H), 7.30-7.35 (*m*, 5H), 7.12 (*dd*, J_1 = 8.1 Hz, J_2 = 2.1 Hz, 2H), 6.77 (*d*, J = 8.4 Hz, 1H), 6.67 (*d*, J = 8.7 Hz, 1H), 5.59 (*s*, 2H), 4.03 (*s*, 3H), 3.82 (*s*, 3H)); ^{13}C-NMR (125 MHz, DMSO-*d6*): 155.2, 154.4, 149.4, 142.0, 138.6, 136.5,

128.8, 127.5, 127.1, 125.9, 119.5, 116.6, 115.6, 113.8,112.1, 110.5, 106.0, 105.3, 56.5, 55.7, 48.0.

3-(1-(2-Chlorobenzyl)-5-(trifluoromethyl)-1*H*-benzo[*d*]imidazol-2-yl)-5,8-dimethoxynaphthalen-1-ol (50): Yield 87% as white solid; mp 183-185°C; IR (KBr) ν_{max}:3352, 2927, 2852, 1745, 1619, 1501, 1442, 1395, 1330, 1256, 1157, 1105, 1053, 934, 805, HR-ESI-MS found *m/z* 513.1192 $[M+H]^+$ (calcd. 513.1193, $C_{27}H_{21}N_2O_3ClF_3$)); ^{1}H-NMR (500 MHz, DMSO-*d6*): 9.66 (*s*, 1H, OH), 7.76 (*d*, J = 8.5 Hz, 1H), 7.74 (*d*, J = 2.0 Hz, 1H), 7.62 (*dd,* J_1 = 4.0 Hz, J_2 = 1.5 Hz, 1H), 7.60 (*dd,* J_1 = 3.5 Hz, J_2 = 1.0 Hz, 1H), 7.38 (*td,* J_1 = 8.5 Hz, J_2 = 1.5 Hz, 1H), 7.27 (*td,* J_1 = 7.5 Hz, J_2 = 1.0 Hz, 1H), 7.21 (*d*, J = 1.5 Hz, 1H), 6.96 (*d*, J = 8.5 Hz, 1H), 6.88 (*d*, J = 8.5 Hz, 1H), 6.68 (*dd,* J_1 = 7.5 Hz, J_2 = 1.0 Hz, 1H), 5.74 (*s*, 2H), 3.98 (*s*, 3H), 3.77 (*s*, 3H)); ^{13}C-NMR (125 MHz, DMSO-*d6*): 155.1, 154.4, 149.41, 149.38, 142.0, 138.7, 133.8, 131.8, 129.7,129.3, 127.9, 127.2, 127.0, 126.8, 119.6, 116.8, 115.6, 113.3, 111.9, 110.4, 106.1, 105.3, 56.5, 55.6, 46.5.

Biological methods

Cell culture and reagents: Vero (ATCC CCL-81) and Huh-7 cells (JCRB Cell Bank, JCRB-0403) were maintained in Dulbecco's Modified Eagle's Medium (DMEM) supplemented with 10% fetal bovine serum, 1% penicillin and streptomycin (P/S) (GIBCO #11995-065), and 2 mM L-glutamine (GIBCO #11500626). MPA was purchased from Sigma (#sig-sml0284-10). H9 human embryonic stem cell-derived cells were purchased from Invitrogen (#N7800-100). Cell cultures and human neural stem cells were maintained and expanded according to the manufacturer's protocol.[25]

Virus preparation: The African ZIKV strain (MR766) was purchased from ATCC (USA, VR-1838). The Asian ZKIV strain was isolated from a patient in New Caledonia (NC-2014-843).[26] Viral stocks were amplified in Vero cells (ATCC, Manassas, USA) and quantified according to the standard plaque assay methodology.[27] Viral stock titers were determined by plaque assay on Vero cells. The quantity of the viral stock was also confirmed by RT-PCR using primers for NS1 regions (5'-TGACTCCCCTCGTAGACTG-3' and 3'-CTCTCCTTCCACTGATTTCCAC-5').

Immunofluorescence analysis: ZIKV infection was evaluated using immunofluorescence analysis (IFA). Cells were fixed with 4% paraformaldehyde, permeabilized using phosphate-buffered saline with 0.1% TritonX-100, and blocked using 2.5% bovine serum albumin (BSA). Mouse monoclonal α-E (4G2)23, purchased from ATCC (# HB-112),[28] was diluted in 2.5% BSA and incubated with cells for 2 h. Secondary antibody goat anti-mouse Alexa488 (Life Technologies, #A28175) and nuclear stain were used at a dilution of 1:1500 in 2.5% BSA. For 384-well plates, six fields per well were imaged using the 10× objective on a PerkinElmer Opera High Content Imaging System (Perkin-Elmer, Waltham, MA, USA), and images were analyzed using in-house imaging software.[29] Percent inhibition was calculated using values of maximum infectivity and background derived from infected cultures treated with 1% DMSO (0% inhibition) and the EC_{100} of positive controls (100% inhibition) as references using the following formula: (DMSO - sample) / (DMSO - EC_{100}) × 100%.[30] The antiviral activity of tested compounds was evaluated by DRC analysis, and EC_{50} and CC_{50} values were calculated using Prism v5.0 software (GraphPad Software, Inc., La Jolla, CA, USA). Experiments were conducted in triplicate with at least three independent repetitions. Cell viability was assessed by determining the total number of Hoechst 33342-stained cells.

Compound screening: Huh-7 cells were seeded in 384-well black wall optical bottom plates (Sigma, CLS3828) in DMEM supplemented with 10% fetal bovine serum and 1% P/S overnight. Cells were pre-treated with tested compounds dissolved in DMSO and further diluted in DMEM in a 1:3 serial dilution at 10 concentrations in triplicate for 1 h at 37°C. Approximately 1 h after compound pre-treatment, 15 µL ZIKV inoculum (MOI 0.8) was added to each well (final volume 50 µL). Infected cells were incubated until 24 hpi at 37°C in an incubator followed by 4% paraformaldehyde fixation and IFA.

Evaluation of anti-ZIKV activity in human neural stem cells: Cells were plated in 384-well format for 18 h before infection. For neural stem cells, plates were coated with poly-L-ornithine (Sigma, P4957) and laminin (Sigma, L2020) 1 day before plating cells. Cells were pre-treated with compounds in a 3-fold serial dilution with 10 concentrations prior to infection of ZIKV MR766 with a MOI of 10. Cells were fixed at 72 hpi, and ZIKV infection was evaluated by IFA. EC_{50} (µM), CC_{50} (µM), and SI values were calculated by DRC analysis in triplicate.

Plaque assay: Vero cells were cultured in growth medium as described above. Cells were incubated with ZIKV for 1 h, washed, and overlaid with a mixture of 1% (w/v) agar (Sigma) and 1% MEM. The assay was terminated by fixing cells with 37% formaldehyde for 4 h. After fixation, the overlay was removed and stained with 1× crystal violet to count ZIKV plaques. Infectious virus titer (PFU/mL) was determined using the following formula: number of plaques × dilution factor × (1 / inoculation volume).

Time-of-addition study: Time-of-addition experiments were conducted as previously reported.[31] Briefly, Huh-7 cells at passage 1 (p1) were plated in 384-well format for 18 h (t = 18 h). Cells were infected at a MOI of 10 at 4°C and then washed at 1.5 hpi. Compounds were treated at different time points as indicated. At 30 hpi, the supernatant of p1 cells was transferred to naïve Huh-7 cells (p2). p1 cells were fixed and evaluated by IFA. p2 cells infected at 24 hpi were fixed and stained.

Cell viability: Cell viability due to CPEs and compound cytotoxicity was assessed using a CellTiter-Glo cell viability kit (Promega, G7570). To examine cytopathic effects, Vero cells were plated in a 384-well white plate for 18 h. Cells were treated with compounds prior to ZIKV infection at a MOI 0.2. Cells were analyzed using the kit at 3 dpi. Percent inhibition was calculated using values of maximum infectivity and background derived from infected cultures treated with 0.5% DMSO (0% inhibition) and the EC_{100} of MPA (100% inhibition) as references using the following formula: (DMSO - sample) / (DMSO - EC_{100}) × 100. To test compound cytotoxicity, Huh-7 cells were plated in a 384-well plate for 18 h. Cells were treated with different concentrations (12.5-200 µM) for 30 h and assayed using CellTiter-Glo.

Graphs and statistics: Prism v5.0 (GraphPad Software Inc., La Jolla, CA) software was used to prepare graphs, calculate EC_{50} and CC_{50} values, and determine statistical significance.

Acknowledgements

This research was funded by the Vietnam National Foundation for Science and Technology Development (104.01-2018.51) and a National Research Foundation of Korea (NRF) grant funded by the Korean government (MSIT, NRF-2017M3A9G6068246).

Conflict of interest

The authors declare no conflict of interest.

Keywords: Zika virus • phenotypic screening • benzimidazoles, sodium metabisulfite • o-phenylenediamine • aldehydes • antivirals • replication

References:

[1] a) S. A. Rasmussen, D. J. Jamieson, M. A. Honein, L. R. Petersen, *N. Engl. J. Med.* **2016**, *374*, 1981-1987; b) J. Lei, G. Hansen, C. Nitsche, C. D. Klein, L. Zhang, R. Hilgenfeld, *Science* **2016**, *353*, 503-505.
[2] S. K. Desai, S. D. Hartman, S. Jayarajan, S. Liu, G. I. Gallicano, *Am. J. Stem Cells* **2017**, *6*, 13-22.
[3] K. Rausch, B. A. Hackett, N. L. Weinbren, S. M. Reeder, Y. Sadovsky, C. A. Hunter, D. C. Schultz, C. B. Coyne, S. Cherry, *Cell Rep.* **2017**, *18*, 804-815.
[4] Y. K. Yoon, M. A. Ali, A. C. Wei, T. S. Choon, R. Ismail, *Eur. J. Med. Chem.* **2015**, *93*, 614-624.
[5] N. T. Chandrika, S. K. Shrestha, H. X. Ngo, S. Garneau-Tsodikova, *Bioorg. Med. Chem.* **2016**, *24*, 3680-3686.
[6] R. Iemura, T. Kawashima, T. Fukuda, K. Ito, G. Tsukamoto, *J. Med. Chem.* **1986**, *29*, 1178-1183.
[7] M. Mader, A. de Dios, C. Shih, R. Bonjouklian, T. Li, W. White, B. L. de Uralde, C. Sánchez-Martinez, M. del Prado, C. Jaramillo, *Bioorg. Med. Chem. Lett.* **2008**, *18*, 179-183.
[8] A. Rao, A. Chimirri, E. De Clercq, A. M. Monforte, P. Monforte, C. Pannecouque, M. Zappalà, *IL Farmaco* **2002**, *57*, 819-823.
[9] a) L. Delang, M. Froeyen, P. Herdewijn, J. Neyts, *Antiviral Res.* **2012**, *93*, 30-38; b) H. I. El Diwani, H. T. Abdel-Mohsen, I. Salama, F. A. F. Ragab, M. M. Ramla, S. A. Galal, M. M. Abdalla, A. Abdel-Wahab, M. A. El Demellawy, *Chem. Pharm. Bull.* **2014**, *62*, 856-866; c) K. Ding, A. Wang, M. A. Boerneke, S. M. Dibrov, T. Hermann, *Bioorg. Med. Chem. Lett.* **2014**, *24*, 3113-3117.
[10] a) Y. K. Yoon, M. A. Ali, A. C. Wei, A. N. Shirazi, K. Parang, T. S. Choon, *Eur. J. Med. Chem.* **2014**, *83*, 448-454; b) K. Y. Yeong, M. A. Ali, C. W. Ang, S. C. Tan, H. Osman, *Tetrahedron Lett.* **2014**, *55*, 4697-4700.
[11] H. Siddiqui, R. Farooq, B. P. Marasini, R. Malik, N. Syed, S. T. Moin, M. I. Choudhary, *Bioorg. Med. Chem.* **2016**, *24*, 3387-3395.
[12] P. Roy, A. Pramanik, *Tetrahedron Lett.* **2013**, *54*, 5243-5245.
[13] J. R. Gillard, P. L. Beaulieu, *Organic Syntheses* **2012**, *89*, 131-142.
[14] a) Y. K. Yoon, M. A. Ali, A. C. Wei, T. S. Choon, H. Osman, K. Parang, A. N. Shirazi, *Bioorg. Med. Chem.* **2014**, *22*, 703-710; b) Y. K. Yoon, M. A. Ali, A. C. Wei, T. S. Choon, K. Y. Khaw, V. Murugaiyah, H. Osman, V. H. Masand, *Bioorg. Chem.* **2013**, *49*, 33-39; c) S. Ahn, Y. B. Cha, M. Kim, K. H. Ahn, Y. C. Kim, *Synth. Met.* **2015**, *199*, 8-13; d) D. Karthik, K. J. Thomas, J. H. Jou, Y. L. Chen, *Dyes Pigm.* **2016**, *133*, 132-142.
[15] B. T. B. Hue, H. M. Nguyen, M. Van Hieu, D. L. D. Thanh, N. H. Son, T. Q. De, H. Morita, *Heterocycles* **2019**, *98*, 650-665.
[16] D. N. Kommi, P. S. Jadhavar, D. Kumar, A. K. Chakraborti, *Green Chem.* **2013**, *15*, 798-810.
[17] H. T. B. Bui, Q. T. K. Ha, W. K. Oh, D. D. Vo, Y. N. T. Chau, C. T. K. Tu, E. C. Pham, P. T. Tran, L. T. Tran, H. V. Mai, *Tetrahedron Lett.* **2016**, *57*, 887-891.
[18] a) M. Tonelli, G. Paglietti, V. Boido, F. Sparatore, F. Marongiu, E. Marongiu, P. La Colla, R. Loddo, *Chem. Biodivers.* **2008**, *5*, 2386-2401; b) R. Raut, H. Beesetti, P. Tyagi, I. Khanna, S. K. Jain, V. U. Jeankumar, P. Yogeeswari, D. Sriram, S. Swaminathan, *Virol. J.* **2015**, *12*, 16.
[19] H. Tang, C. Hammack, S. C. Ogden, Z. Wen, X. Qian, Y. Li, B. Yao, J. Shin, F. Zhang, E. M. Lee, K. M. Christian, R. A. Didier, P. Jin, H. Song, G. L. Ming, *Cell Stem Cell* **2016**, *18*, 587-590.
[20] R. Delvecchio, L. M. Higa, P. Pezzuto, A. L. Valadao, P. P. Garcez, F. L. Monteiro, E. C. Loiola, A. A. Dias, F. J. Silva, M. T. Aliota, E. A. Caine, J. E. Osorio, M. Bellio, D. H. O'Connor, S. Rehen, R. S. de Aguiar, A. Savarino, L. Campanati, A. Tanuri, *Viruses* **2016**, *8*, 322.
[21] a) P. Österlund, M. Jiang, V. Westenius, S. Kuivanen, R. Järvi, L. Kakkola, R. Lundberg, K. Melén, M. Korva, T. Avšič–Županc, *Sci. Rep.* **2019**, *9*, 1-15; b) K. Esser-Nobis, L. D. Aarreberg, J. A. Roby, M. R. Fairgrieve, R. Green, M. Gale, *J. Virol.* **2019**, *93*, e00640-00619.
[22] a) D. Udenze, I. Trus, N. Berube, V. Gerdts, U. Karniychuk, infections, *Emerging Microbes Infect.* **2019**, *8*, 1098-1107; b) Q. Shao, S. Herrlinger, Y.-N. Zhu, M. Yang, F. Goodfellow, S. L. Stice, X.-P. Qi, M. A. Brindley, J.-F. Chen, *Development* **2017**, *144*, 4114-4124.
[23] C. Xie, X. Han, J. Gong, D. Li, C. Ma, *Org. Biomol. Chem.* **2017**, *15*, 5811-5819.
[24] J. E. Sadig, R. Foster, F. Wakenhut, M. C. Willis, *J. Org. Chem.* **2012**, *77*, 9473-9486.
[25] M. I. Onyshchenko, I. G. Panyutin, I. V. Panyutin, R. D. Neumann, *Stem Cells Int.* **2012**, *2012*, 634914.
[26] E. Calvez, O. O'Connor, M. Pol, D. Rousset, O. Faye, V. Richard, A. Tarantola, M. Dupont-Rouzeyrol, *Emerging Microbes Infect.* **2018**, *7*, 159.
[27] J. A. Bernatchez, Z. Yang, M. Coste, J. Li, S. Beck, Y. Liu, A. E. Clark, Z. Zhu, L. A. Luna, C. D. Sohl, B. W. Purse, R. Li, J. L. Siqueira-Neto, *Antimicrob. Agents Chemother.* **2018**, *62*, e00725-00718.
[28] D. Shum, J. L. Smith, A. J. Hirsch, B. Bhinder, C. Radu, D. A. Stein, J. A. Nelson, K. Fruh, H. Djaballah, *Assay Drug Dev. Technol.* **2010**, *8*, 553-570.
[29] C. Ko, W. J. Park, S. Park, S. Kim, M. P. Windisch, W. S. Ryu, *Antiviral Ther.* **2015**, *20*, 835-842.
[30] M. Lee, J. Yang, E. Jo, J. Y. Lee, H. Y. Kim, R. Bartenschlager, E. C. Shin, Y. S. Bae, M. P. Windisch, *Sci. Rep.* **2017**, *7*, 44676.
[31] a) J. Zmurko, R. E. Marques, D. Schols, E. Verbeken, S. J. Kaptein, J. Neyts, *PLoS Neglected Trop. Dis.* **2016**, *10*, e0004695; b) M. Lee, J. Yang, S. Park, E. Jo, H. Y. Kim, Y. S. Bae, M. P. Windisch, *Antiviral Res.* **2016**, *132*, 287-295.

Entry for the Table of Contents

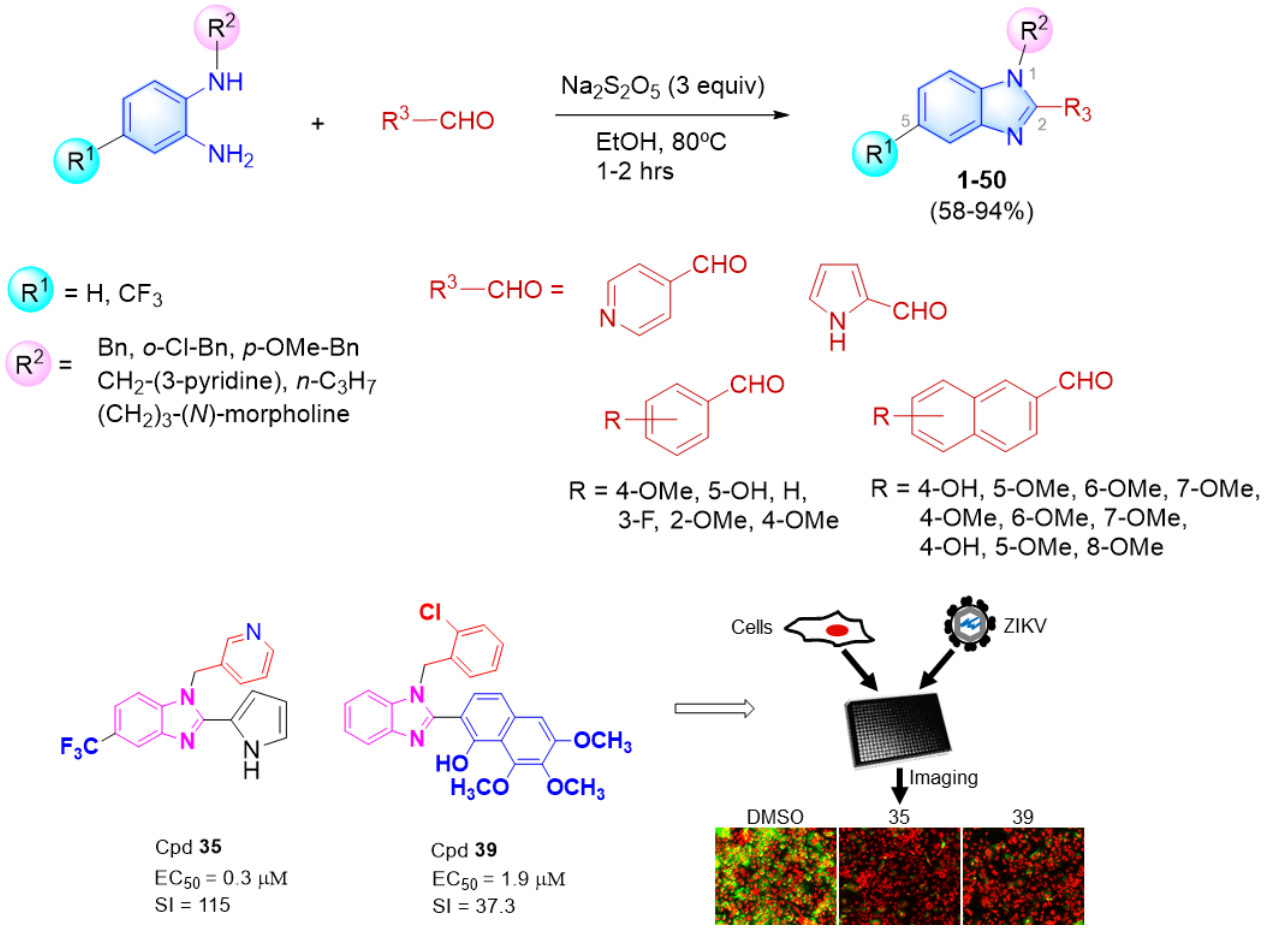

First report of 1,2-disubstituted benzimidazole (BMZ) derivatives as potent Zika virus (ZIKV) inhibitors. BMZs were synthesized through an efficient and environmentally friendly one-pot condensation between 1,2-phenylenediamines and aromatic aldehydes utilizing inexpensive and non-toxic inorganic salt sodium metabisulfite. *In vitro* screening of 50 1,2-disubstituted BMZ derivatives showed their ability to interfere with ZIKV infection in human neural stem cells. Compound **39** displayed the highest antiviral efficacy against the African ZIKV strain in term of selectivity index (SI) in Huh-7 (SI>37) and neural stem cells (SI=12), whereas compound **35** possessed the highest activity against the Asian ZIKV strain (SI=115) in Vero cells. Furthermore, a time-of-addition study indicated that BMZs inhibit ZIKV RNA replication.